# THE EFFECTS OF SEQUENCE CHARACTERISTICS ON COMPETITIVE HYBRIDIZATION KINETICS

A Thesis

Presented to

The Academic Faculty

by

Gita Mahmoudabadi

In Partial Fulfillment

of the Requirements for Undergraduate

Research Option

Georgia Institute of Technology

August, 2010

# THE EFFECTS OF SEQUENCE CHARACTERISTICS ON COMPETITIVE HYBRIDIZATION KINETICS

Approved by

Dr. Valeria Tohver Milam, Assistant Professor
School of Material Science and Engineering
*Georgia Institute of Technology*

Dr. Paul J. Benkeser, Associate Chair for Undergraduate Studies
Department of Biomedical Engineering
*Georgia Institute of Technology*

Date Approved: Fall, 2010

"Life is just a three-letter word."

Carl Sagan and Ann Druyan, *Shadows of Forgotten Ancestors*

# ACKNOWLEDGEMENTS

I am truly grateful to my research advisor, Dr. Valeria Milam, and my research mentor Dr. Bryan Baker who have guided me through my undergraduate research experience with great patience and encouragement. I would like to thank all other members of the Milam Lab, especially James Hardin, for offering me their unique and valuable insight.

# TABLE OF CONTENTS

Page

# LIST OF TABLES

Page

# LIST OF FIGURES

Page

# LIST OF SYMBOLS AND ABBREVIATIONS

| | |
|---|---|
| DNA | deoxyribonucleic acid |
| RNA | ribonucleic acid |
| A | adenine |
| T | thymine |
| G | guanine |
| C | cytosine |
| U | uracil |

# SUMMARY

DNA and RNA profiling technologies have a promising role in elucidating the genetic component of various pathological conditions such as human cancers. The increasing demand for such technologies has motivated research into the design of highly sensitive, accurate and cost-efficient nucleic acid detection systems. We employed double-stranded DNA probes, formed by the hybridization of DNA primary targets to single-stranded probes, in order to detect the presence of targets in solution via competitive hybridization events. In our approach, displacement of the original hybridization partner is driven by the affinity differences of the primary and the competitive target for the immobilized strand. Hence, unlike conventional nucleic acid detection technologies such as microarrays, which rely on elevated temperatures for improved detection specificity, our system design imposes specificity at isothermal, room temperature conditions. We report our investigation of competitive hybridization kinetics as a function of double-stranded sequence in which the parameters of length and base-pair mismatch are used to tune affinity of the double-stranded probes. Better understanding of competitive hybridization kinetics will aid the development of highly specific nucleic acid detection systems.

# INTRODUCTION

A better understanding of the expression of numerous genes, their biological functions as regulators of healthy or malignant cellular phenotypes, promises more effective diagnosis, prognosis and treatment strategies for various pathological states. RNA profiling technologies are of particular interest in elucidating mechanisms of action of disease genes (Golub, 2007). With ˜22,000 protein-coding transcripts, sequences of messenger RNA provide disease specific signatures for classifying a wide variety of human cancers (Ramaswamy, 2001).

The compilation of large-scale genetic and proteomic libraries, however, require high-throughput, cost-efficient, and highly sensitive nucleic acid detection systems (Golub, 2007). Of the many nucleic acid detection schemes, microarrays are the most prominent; however, the simplicity of microarray technology is compromised due to the various temperature protocols necessary to promote greater detection specificity. Microarrays utilize a single hybridization step between a dye-modified target sequence and a complementary probe sequence. In some cases this direct hybridization event may not differentiate perfectly-matched and mismatched duplexes (Koltai, 2008). Labeling biases that result from the chemical modification of targets can also make quantification less accurate (Epstein, 2002). Additionally, the high costs of microarrays have hindered extensive testing of reliability and validity (Li, 2002). Moreover, given the high costs of microarray fabrication, custom-designed arrays for analyzing an individual expression profile is impractical in many instances (Golub, 2007).

Introducing structural modifications such as hairpins (DeRisi, J., 1996), minor groove-binding groups (Nicewarner-Pena, S.R., 2001) or peptide nucleic acids (Chan, W.C., 2002) in probes would increase the specificity of microarrays but would reduce both the simplicity and the cost-efficiency of probe preparation (Li, 2002). On the other hand, using double-stranded probes (dsProbes), formed by the hybridization of primary targets to single-stranded probes, allows for detection events of high specificity at room temperature conditions. To favor displacement of one strand in the dsProbe, which signifies a detection event, the secondary or the "competitive" targets must have a greater affinity for the probe than the primary target. These probes can discriminate between a perfectly matched target and targets containing a mismatch, which is ideal for various applications in molecular diagnostics especially in genotyping and mutation detection (Li, 2002). In light of the great demand for RNA profiling techniques, we report the use of unlabeled RNA target in addition to several DNA targets as competitive partners for the double-stranded DNA probes, and monitor the kinetics of the competitive hybridization reaction. Optimizing parameters such as target length and base-pair mismatch in the competitive hybridization studies provides insight towards successful development of highly specific and cost-efficient nucleic acid detection schemes. Furthermore, we employ microsphere-based substrates for all hybridization events since microspheres have the benefits of ease of use, low cost, and more flexibility than conventional planar arrays (Dunbar, 2006).

# MATERIALS AND METHODS

***Materials.*** 1.0 ìm carboxylate modified latexes (CML) were purchased from Bangs Laboratories (Fishers, IN). All oligonucleotide strands were purchased from Integrated DNA Technologies (IDT, Coralville, IA). Sequence synthesis and modification as well as HPLC purification processes were performed by the supplier. The DNA probe sequence were amine functionalized and contained 12 carbon-based molecules to separate the amine group from the hybridizing bases. Perfectly complementary primary targets as well as those containing a center mismatch were fluorescein-labeled at the 5' end via a modified thymine. Perfectly complementary competitive targets as well as those with mismatches at the center or at the third base (from the 3' end) were not labeled. Target sequences were of 11, 13, or 15 base pairs in length. After purchase, all oligonucleotide strands were stored in 100 ìM aliquots at -20 °C. Fluorescein-labeled (primary targets) and unlabeled (competitive targets) oligonucleotides were stored in Tris/EDTA at pH 8.0 and 7.4, respectively.

***Buffer Preparation***. PBS/Tween buffer was made by mixing 45.0 mL of nanopure $H_2O$, 100.0 ìL of Tween 20 (Calbiochem, EMD Biosciences, La Jolla, CA) and 5.0 mL of 10x PBS concentrate (Sigma, St. Louis, MO). The solution was mixed by end-over-end mixing for one hour and then filtered using a 0.2 ìm syringe cap filter. The coupling buffer contained 0.05% Proclin 300 and 50 mM 2-(*N*-morpholino)ethanesulfonic acid (MES). It was titrated to a pH of 5.2 in nanopure water. All buffers were made with DIamond Nanopure water (Barnstead International, Dubuque, IA).

***Conjugation of DNA Probes to Microspheres.*** Using *N*-Ethyl-*N'*-(3-dimethylaminopropyl) carbodiimide hydrochloride (EDAC**)** (Sigma, St. Louis, MO), DNA probes were conjugated to the surface of microparticles as follows (Liu, 2005). 25.0 ìL of CML 1.0 ìm particles at 4% solids were centrifuged and resuspended in 100 ìL of coupling buffer. After a second centrifugation step, the bead pellet was resuspended in 150 ìL of coupling buffer. 50.0 ìL of coupling buffer was then added to 10 mg of pre-weighed and $N_2$ backfilled EDAC and vortexed. 25.0 ìL of EDAC/coupling buffer solution was added to the particle suspension along with 200.0 ìL of 10 ìM DNA probe solution. The suspension was vortexed and mixed end-over-end for 2 hours, after which probe-conjugated particles were washed two times and resuspended in 100.0 ìL of PBS/Tween at a final concentration of 1% solids. All wash steps comprised of centrifugation (at 9.1 x 1000g for 2 minutes), and resuspension of particle pellet in PBS/Tween buffer followed by vortexing.

***Primary Hybridization.*** 12.0 ìL of the probe-conjugated particles and 188.0 ìL of PBS/Tween were briefly mixed, sonicated, centrifuged and resuspended in 200.0 ìL of PBS/Tween. 200.0 ìL of primary target at 10 ìM concentration was added to the suspension which was then briefly vortexed. The final suspension volume was 400 ìL with a 5 ìM total concentration of primary target DNA. Addition of the primary target to suspension marked the start time of the primary hybridization reaction. The reaction continued for 6 hours while undergoing end-over-end mixing. Subsequent to two washes at the end of primary hybridization, the particles were resuspended in 400.0 ìL of PBS/Tween. 20.0 ìL of this suspension was removed and diluted to a final volume of 100.0 ìL in PBS/Tween and following two wash steps, it was stored at 4-8 °C until flow

cytometry. This sample was collected as a reference sample referred to as the zero time point sample.

***Competitive Hybridization.*** For competitive hybridization studies, the volume of the suspension was restored to 400.0 ìL by adding 20.0 ìL of 100 ìM competitive target or 20.0 ìL of Tris/EDTA (pH 8) depending on whether the kinetics of competitive hybridization or dissociation were under investigation, respectively. The addition of the competitive target marked the start time of the competitive hybridization reaction. The suspension was then vortexed and mixed end-over-end for 72 hours, throughout which 40.0 ìL samples were obtained at 0.25, 0.5, 0.75, 1, 6, 24, 48 and 72 hours with respect to the reaction start time. At each time point, the sample was added to 60.0 ìL of PBS/Tween for a total volume of 100.0 ìL and after two wash steps, it was stored at 4-8 °C until flow cytometry.

***Flow Cytometry.*** To quantify the density of dsProbes, flow cytometry was performed on samples from all time points. 100.0 ìL samples were diluted with 900.0 ìL of PBS/Tween to a total volume of 1.0 mL. To serve as a negative control (non-fluorescent sample), 2.0 ìL of coupled microparticles was washed two times and diluted to 1.0 mL with PBS/Tween. FITC high fluorescence intensity standards along with the calibration sheet from Bangs Laboratories (Fishers, IN) were used to convert measured fluorescence intensity values into dsProbe density values. Flow cytometry measurements were obtained using a Becton Dickinson FACS II flow cytometer (Becton Dickinson, San Jose, CA).

# RESULTS AND DISCUSSION

Competitive hybridization can be defined as a competition between two oligonucleotides due to their affinity for hybridization to a complementary nucleic acid sequence. The versatility of competitive hybridization in various fields of biotechnology such as in drug-delivery, gene silencing, DNA-based computing and nanodevices has become increasingly evident: synthetic riboregulators for use in post-transcriptional gene regulation (Isaacs, 2004), DNA catalytic gate design in modular molecular circuits (Qian, 2009), DNA molecular nanomotor for thrombin detection (Li, 2002), and controlled disassembly of colloidal satellites for novel drug-delivery applications (Tison, 2009; Parpart, 2010) are only a few of the many studies that have used competitive hybridization. We employed competitive hybridization within the context of nucleic acid detection to construct an isothermal detection scheme on microparticle platform. In our system the competitive target has a higher affinity for the immobilized strand and therefore displaces the primary target that is fluorescently labeled.

Since the primary target is fluorescently labeled, the fluorescence intensity of microparticles correlates with the number of dsProbes chemically bound to their surface. With this information, dsProbe density values are measured. The dsProbe density at the zero time point of the competitive hybridization reaction, prior to addition of competitive target, is referenced to as the original dsProbe density. The competitive hybridization reaction is initiated when the competitive target is introduced to the suspension of microparticles with immobilized dsProbes. Due to its ability to form a duplex of greater thermodynamic stability than the original dsProbe, the competitive target drives the

displacement of the fluorescently labeled primary target; the subsequent decrease in the fluorescence intensity can be recorded as a quantifiable, detection event. Using this displacement-based approach to detect oligonucleotides eliminates the need for 1) temperature protocols necessary for increased detection specificity, as depicted in Figure 1, and 2) the chemical labeling of targets, thereby simplifying the detection procedure.

In the current studies, the loss in fluorescence signal can result from both competitive hybridization as well as thermal dissociation processes since either path contributes to the "release" of dsProbes. The term "displacement," however, refers specifically to signal loss due to competitive hybridization in which one strand is replaced with another. Other nomenclature used to identify the competitive or primary targets is briefly explained in Table 1. DNA primary and competitive targets are denoted by the letter "T", followed by a number representative of the sequence base length. In case of a center mismatch, the letter "m" accompanies the name of sequence. If the mismatch occurs anywhere but at the center of the sequence, "x" will separate the name from the location of the mismatch (with respect to 3' end). For example, T15mx3 is a DNA target of 15 bases in length with a mismatch at its third base. RNA target is identified by "R", and the immobilized sequence is referred to as P15. All dsProbes are indicated using a "P15-target name" format. For example, P15-T13 denotes a DNA dsProbe with 13 base pair matches in length. One dsProbe, P15-T13f, also denotes a DNA dsProbe with 13 base pair matches in length, but the "f" denotes that the orientation of the two unhybridized bases is flipped if compared to P15-T13.

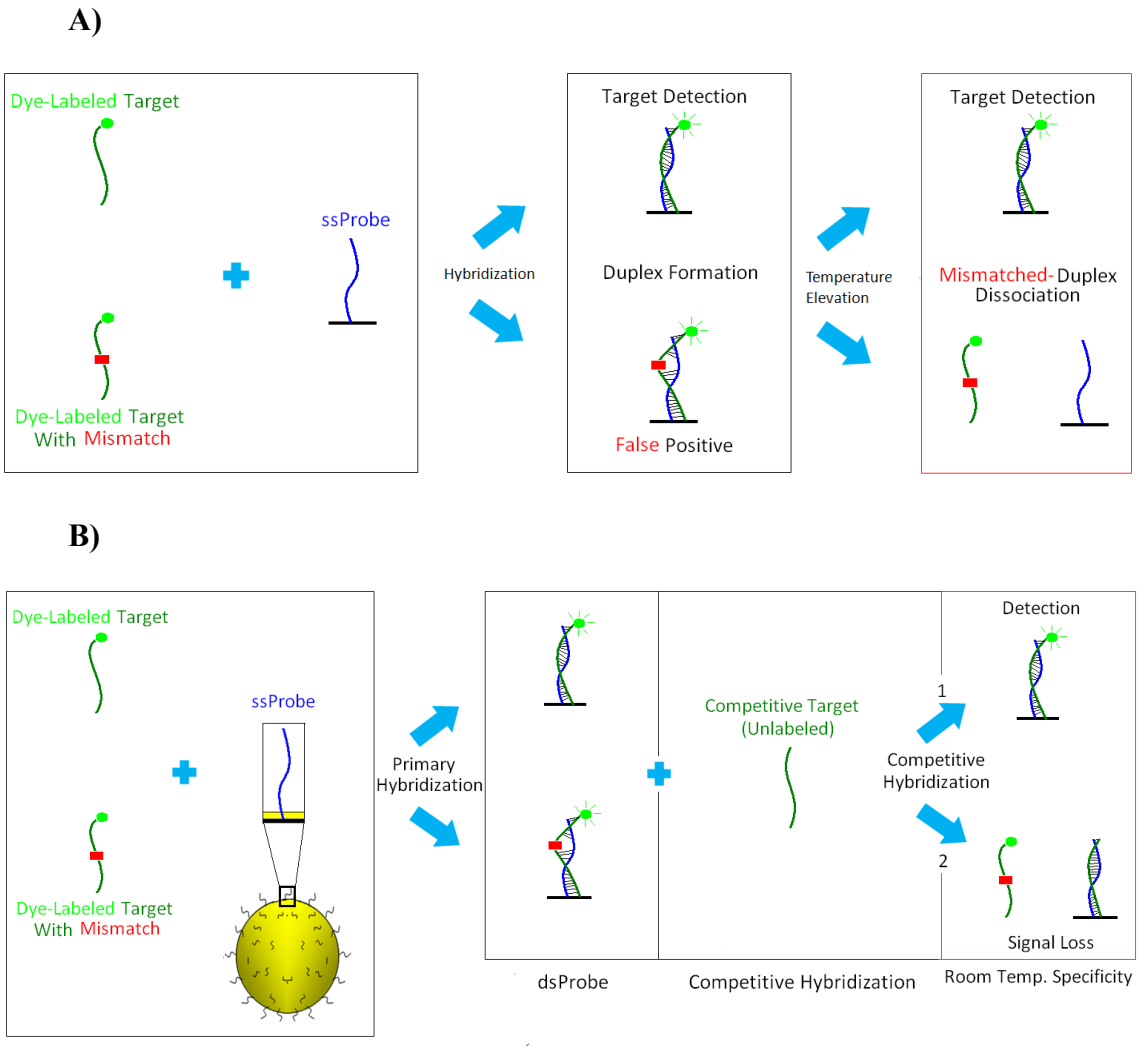


**Figure 1.** Representative schematics highlighting the procedural differences between the single-stranded detection approaches (A) and our double-stranded assay which employs the competitive hybridization reaction on particle surfaces (B). In B, Step 1 (top right) represents an unsuccessful competitive hybridization event whereas step 2 (bottom right) depicts a successful competitive hybridization event. Using competitive hybridization, the need for temperature protocols and labeling of targets is eliminated, while detection event of high specificity is achieved.

**Table 1:** List of sequences employed as immobilized strands (ssProbe) as well as primary and competitive targets. When used as primary target (to form dsProbe), the sequence is labeled with a fluorescein molecule at its 5' end (not shown). The red, underlined letters within the sequence denote the mismatched bases.

| **ssProbe** | |
|---|---|
| P15 | 5' - Amine-(12 carbon) CTC GTC ACA CTA TCA - 3' |
| **dsProbe** | |
| P15-T11 | 5' - Amine-(12 carbon) CTC GTC ACA CTA TCA - 3'<br>3' -AG TGT GAT AGT (T Fluor)- 5' |
| P15-T11m | 5' - Amine-(12 carbon) CTC GTC ACA CTA TCA - 3'<br>3' -AG TGT **C**AT AGT (T Fluor)- 5' |
| P15-T13 | 5' - Amine-(12 carbon) CTC GTC ACA CTA TCA - 3'<br>3' -G CAG TGT GAT AGT (T Fluor)- 5' |
| P15-T13m | 5' - Amine-(12 carbon) CTC GTC ACA CTA TCA - 3'<br>3' -G CAG **A**GT GAT AGT (T Fluor)- 5' |
| P15-T15 | 5' - Amine-(12 carbon) CTC GTC ACA CTA TCA - 3'<br>3' -GAG CAG TGT GAT AGT (T Fluor)- 5' |
| P15-T15m | 5' - Amine-(12 carbon) CTC GTC ACA CTA TCA - 3'<br>3' -GAG CAG T**C**T GAT AGT (T Fluor)- 5' |
| P15-T13f | 5' - Amine-(12 carbon) CTC GTC ACA CTA TCA - 3'<br>3' -(T Fluor) G CAG TGT GAT AGT - 5' |
| **Competitive Targets** | |

| | |
|---|---|
| T15 | 3' - GAG CAG TGT GAT AGT - 5' |
| T15m | 3' - GAG CAG T**C**T GAT AGT - 5' |
| T15mx3 | 3' - GA**C** CAG TGT GAT AGT - 5' |
| R15 | 3' - GAG CAG UGU GAU AGU - 5' |

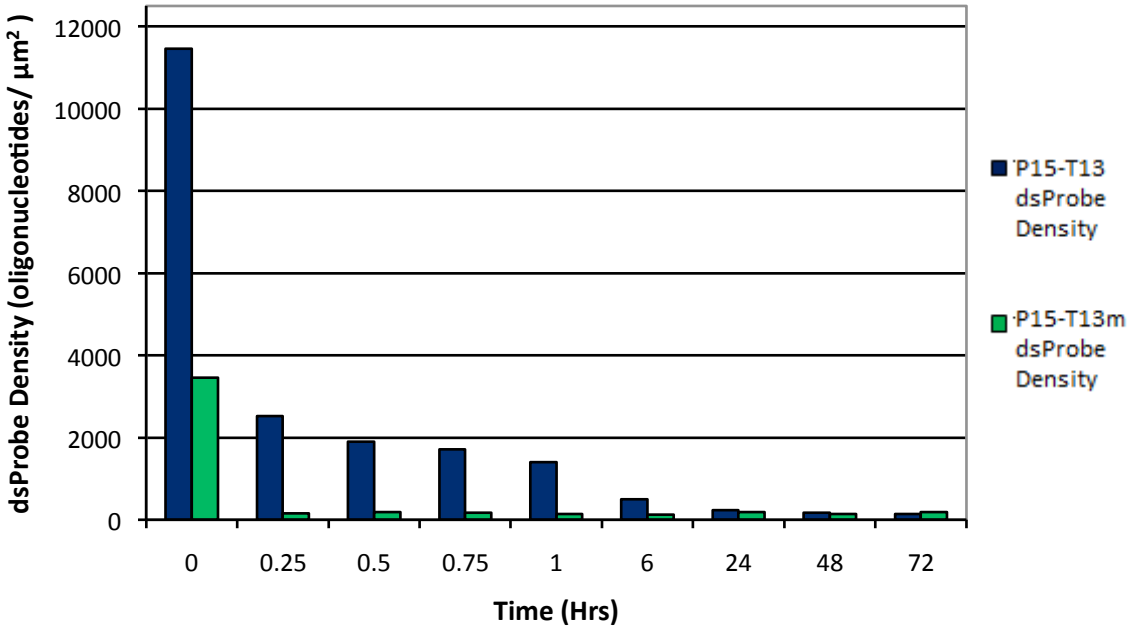


**Figure 2.** dsProbe densities after competitive hybridization reaction between DNA competitive target, T15, and dsProbes: P15-T13 and P15-T13m. The densities of both dsProbes decrease as a function of competitive hybridization reaction time. The density of dsProbe P15-T13 is higher than that of P15-T13m at nearly all time points.

Figure 2 shows the release of the labeled partner strand in 13-base-long dsProbes (P15-T13 and P15-T13m) in the presence of 15-base-long DNA competitive target (T15) and is thus indicative of successful competitive hybridization reactions. According to Gibb's free energy equation (Equation 1), at low temperature conditions such as at room temperature, the Gibb's free energy is primarily governed by enthalpic changes.

$$\Delta G = \Delta H - T \times \Delta S \qquad \mathbf{1}$$

Although in competitive hybridization, the formation of longer duplexes results in an entropic loss, the additional hydrogen bond formations in longer duplexes contribute to an enthalpic gain. The formation of longer duplexes is thus more thermodynamically favorable because the enthalpic gain outweighs the entropic loss, resulting in a net decrease in the free energy of the system.

Whereas P15-T13 dsProbe is a perfectly matched duplex, P15-T13m has a center mismatch. At the end of the primary hybridization reaction, nearly three times more perfectly matched probes than the mismatched probes are formed. A comparison between the original dsProbe densities thus confirms that the inclusion of a center mismatch is a thermodynamically unfavorable factor in primary hybridization or dsProbe formation (Figure 2). Since the original duplex densities varied, depending on the sequence of the dsProbe, subsequent figures will present data as the fraction of partner strands released in order to simplify comparisons.

Figure 3 presents competitive hybridization kinetic profiles of dsProbes P15-T13, P15-T11 and P15-T15m. To demonstrate the viability of our detection scheme in detecting RNA oligonucleotides, 15-bases long RNA competitive target was used (R15). Similar to DNA, the RNA competitive target releases the labeled strand of the dsProbes based on thermodynamic considerations such its ability to form a longer, perfectly-matched duplex. As the competitive hybridization approaches equilibrium by the end of the experiment, the fraction released at the final time point can also be used to compare the thermodynamic stabilities of the dsProbes.

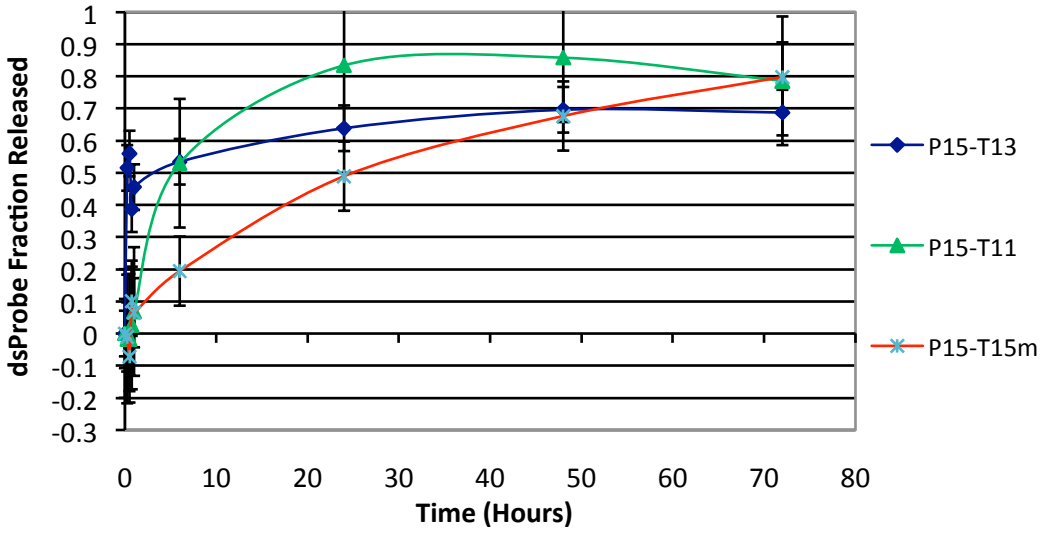


**Figure 3.** The release kinetics of the original hybridization partner from DNA dsProbes P15-T13, P15-T11 and P15-T15m in presence of 15-bases long RNA competitive target (R15). The fraction of partner strands released from the dsProbes increases as a function of competitive hybridization reaction time. The error bars represent the standard error (n = 3).

The fraction of P15-T15m and P15-T11 dsProbes that released their labeled partner strand at the end of competitive hybridization reaction were nearly the same, confirming similar levels of thermodynamic stability for these dsProbes (Figure 3). It could thus be inferred that the contribution of a center base-pairing to duplex stability is comparable to that from four consecutive base pairings at the end of a dsProbe 15 bases long. More generally, even though each hydrogen bond makes a contribution to the overall duplex stability, these contributions need not be equal. The location of mismatched bases within a duplex (e.g. center versus near-end mismatch), for example, may be an important consideration in hybridization or duplex stability. Finally, Figure 3 shows the lowest fraction of release at the end of competitive hybridization reaction occurs for P15-T13 making it the most thermodynamically stable of the three probes. Despite its greater thermodynamic stability, this probe had the fastest release timing with the majority of release occurring within the 6 hours of the competitive hybridization reaction.

Where thermal dissociation was expected to occur in the absence of competitive targets, the results present a vastly different picture. Figure 4 displays negative fractions released in all three profiles, implying an increase in the number of dsProbes on the particle surface. A potential cause for this anomalous trend was proposed to be the wash protocol described in the Experimental Methods.

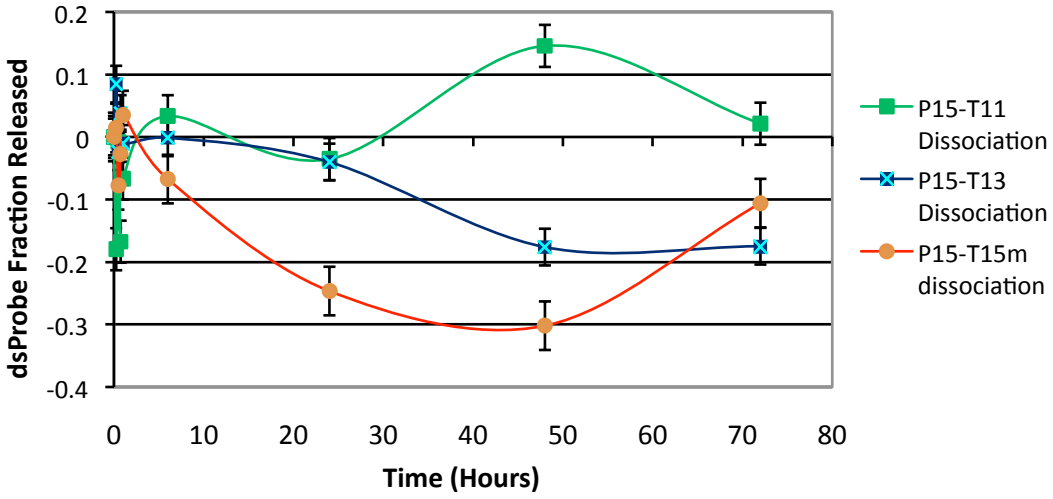


**Figure 4.** Thermal dissociation profiles of dsProbes: P15-T13, P15-T11 and P15-T15m. Negative dsProbe fraction released appear in all three profiles, and the fluctuations in fraction released do not follow an obvious trend. The error bars represent the standard error (n = 3).

To explain this unexpected trend, we suggest that the simultaneous associations of a primary target with multiple ssProbes or the partial hybridizations of multiple primary targets with one ssProbe may occur and lead to the formation of imperfect dsProbes initially as depicted schematically in Figure 5. The two washes at the end of primary hybridization are designed to remove excess primary target as well as the weakly associated partner strands such as imperfectly hybridized dsProbes. Similarly, two washes are performed at each of the competitive hybridization time points. However, the zero time point undergoes a total of four consecutive washes, whereas later time points

undergo two sets of washes spaced by longer incubation time with competitive targets. This subtle difference in handling may contribute to the observed negative dsProbe fraction released. The washes following primary hybridization remove excess targets in solution, thereby creating a concentration gradient that promotes the dissociation of imperfectly hybridized strands into the solution. If allowed enough incubation time before the competitive hybridization washes are performed, these strands may reorganize in more thermodynamically favorable duplex conformations. If incubation time is not allotted between the four washes, such as in the case of the zero time point, then a greater number of imperfectly, hybridized targets will be lost. If the later time points do result in reorganization of imperfect duplexes to more perfect duplexes, then a relative difference in fluorescence may occur between the zero time point and the later time points. Negative fractions of dsProbe release may occur as seen in Figure 4.

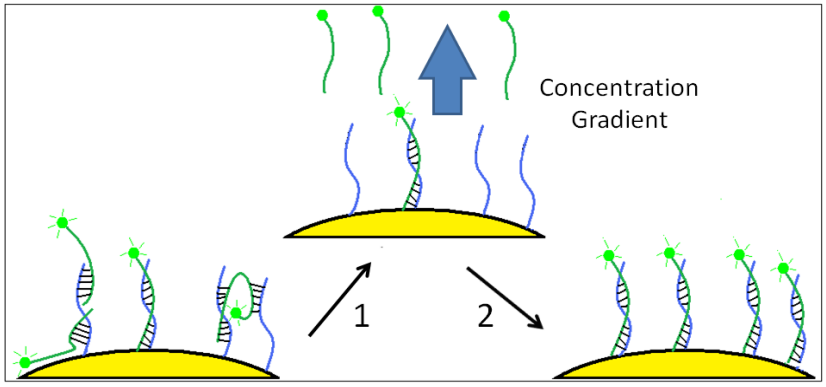


**Figure 5**. A representative schematic of imperfectly hybridized primary targets and their rehybridization upon longer incubation time (prior to washing). Step 1 refers to the wash step that destabilizes imperfectly hybridized dsProbes by creating a concentration gradient. Step 2 represents a longer incubation time during which primary targets form more perfect dsProbes against the concentration gradient.

The release kinetics of dsProbe P15-T15m in presence of various competitive targets were indistinguishable (Figure 6). It was previously theorized that the unhybridized

bases in a dsProbe serve as a nucleation site for the competitive hybridization reaction (Porchke, 1971). These unhybridized bases may thus form a "toehold" region for the competitive target where it first interacts with and bonds to dsProbe and then sequentially displaces the primary target to form a more thermodynamically favorable duplex. P15-T15m is a particularly interesting dsProbe for kinetic studies since it lacks a toehold region.

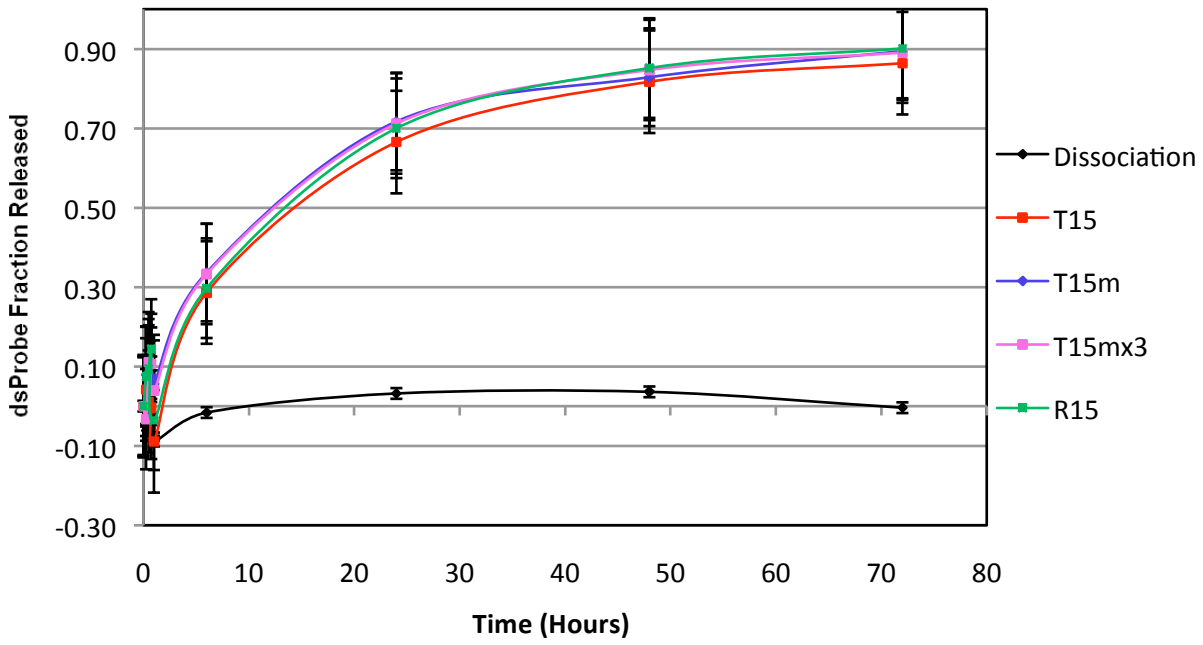


**Figure 6.** The release kinetics of P15-T15m dsProbe in absence of competitive target and in presence of DNA (T15, T15m, T15mx3) or RNA (R15) competitive targets. The release kinetics of P15-T15m, using various competitive targets, were the same. The error bars represent the standard error (n = 3).

The competitive targets were shown to be equally capable of releasing P15-T15m despite their affinity differences for the probe with nearly 90% of original dsProbe released by each competitive target. T15m also displaced nearly all of the original dsProbes. This result may be indicative of the effects of the fluorescein molecule in altering, perhaps even lowering, the affinity of the competitive targets compared to the analogous primary

targets. Moreover, not more than 5% of P15-T15m release can be attributed to thermal dissociation as as presented by the thermal dissociation profile in Figure 7. hese results suggest that P15-T15m is not a preferred choice of dsProbe due to its limited discrimination between the detected competitive targets of similar affinities.

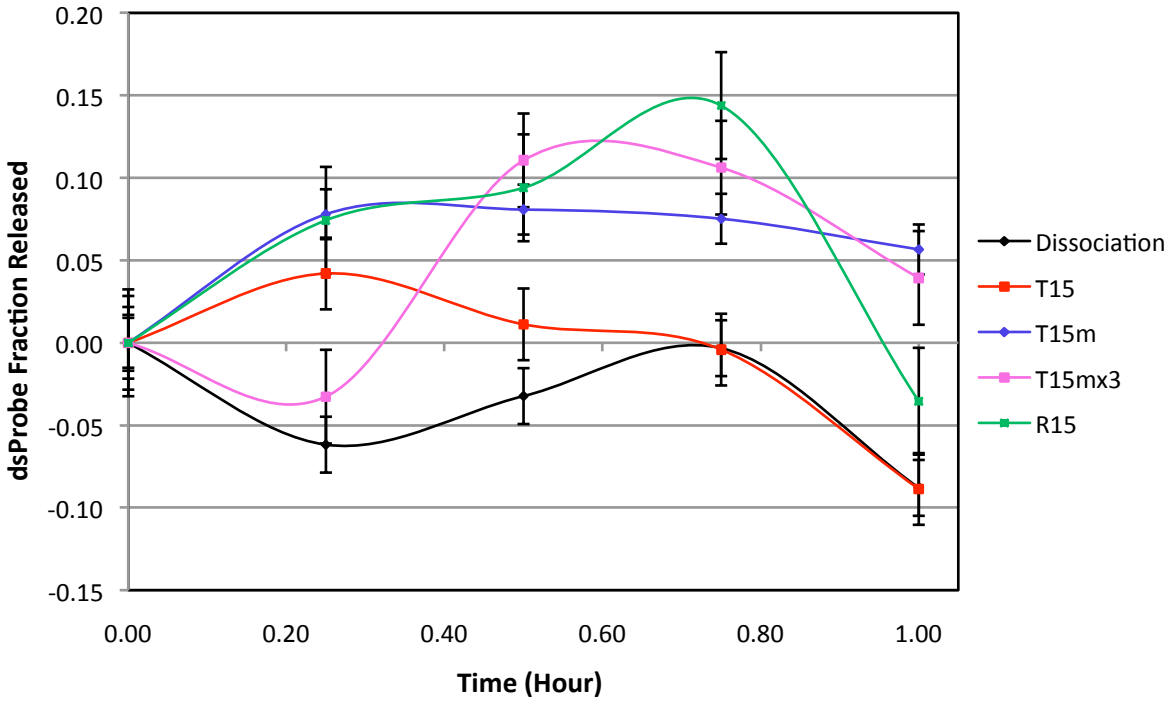


**Figure 7.** The release kinetics of P15-T15m dsProbe in absence of competitive target and in presence of DNA (T15, T15m, T15mx3) or RNA (R15) competitive targets within the first hour of competitive hybridization reaction. The error bars represent the standard error (n = 3).

As shown in Figure 7, within the first of hour of competitive hybridization the reaction is far from equilibrium conditions and negative fractions which could be the result of the wash protocols are apparent within the first six hours of competitive hybridization.

Figure 8 depicts the release kinetics of P15-T13f as a function of various competitive targets. Although the competitive targets used to release P15-T15m and P15-T13f were the same, the release kinetics of the two dsProbes were entirely different. P15-T13f, a

dsProbe of 13 bases in length with its fluorescein molecule located at the 3' end of the primary target, contains two unhybridized bases at the free end of the duplex (unlike P15-T13). These unhybridized bases may serve as a nucleation site for the competitive targets, thereby allowing for a clear discrimination between the competitive targets. In detection and discrimination between targets of similar affinities, P15-T13f is an appropriate dsProbe.

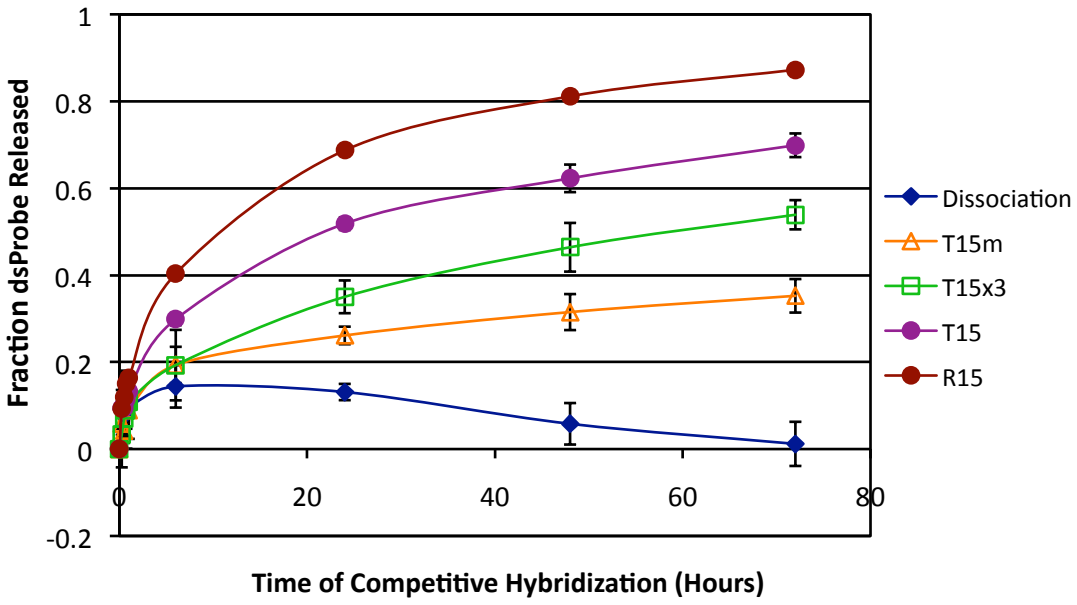


**Figure 8.** The release kinetics of P15-T13f dsProbe in absence of competitive target (dissocation) and in presence of DNA (T15, T15m, T15mx3) or RNA (R15) competitive targets. Variations in release kinetics using competitive targets of differing affinities are apparent. The error bars represent the standard error (n = 3).

As depicted in Figure 8, R15 resulted in the highest amount of primary targets released from the dsProbes (approximately 90%) followed by T15, T15mx3, and T15m. The fraction released at the end of the competitive hybridization reaction is correlated to dsProbe stability in presence of the competitive target. The results indicate that the formation of P15-R15 is the most thermodynamically favorable duplex among those

presented in this study. P15-T15mx3 is more stable than P15-T15m but less stable than P15-T15, which confirms that 1) inclusion of mismatched bases compromises the stability of the duplex, and 2) the location of mismatched base-pair is an important parameter in duplex stability.

Figure 9 presents the release kinetics of P15-T13f within the first hour of the competitive hybridization reaction. The fractions released fluctuates but increases as a function of time. Interestingly, no negative fractions are observed. Hence, imperfect hybridization due to wash protocol may be sequence specific or it may be affected by the orientation of the toehold region within a dsProbe.

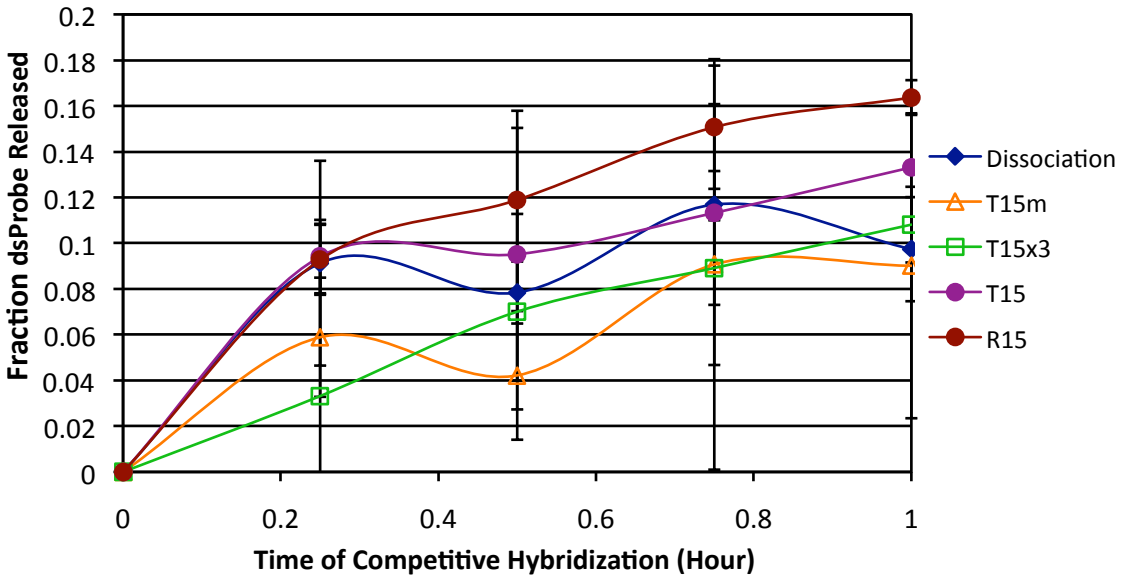


**Figure 9.** The release kinetics of P15-T13f dsProbe in absence of competitive target and in presence of DNA (T15, T15m, T15mx3) or RNA (R15) competitive targets within the first hour of competitive hybridization reaction. The fraction released increases as a function of time. The error bars represent the standard error (n = 3).

# CONCLUSION

In this study we characterize the kinetics of competitive hybridization for several dsProbes and targets. Thermodynamic considerations such as sequence length and inclusion of mismatch allowed us to design dsProbes with enhanced detection specificity over single-stranded probes. Applying a competitive hybridization approach we demonstrated displacement by RNA targets, which holds great promise for RNA detection. By analyzing the kinetics of competitive hybridization, the role of handling protocol in dsProbe formation as well as sequence design of the dsProbe and implications on target discrimination were discussed. These results may aid the design of highly specific and methodologically-simple detection technologies that will further enhance nucleic acid detection systems.

## REFERENCES


Todd R. Golub JL, David Peck, Jun Lu, Eric Alexander Miska, Inventor. Solution-based methods for RNA expression profiling, 2007.

Ramaswamy, S., P. Tamayo, et al. (2001). "Multiclass cancer diagnosis using tumor gene expression signatures." *Proceedings of the National Academy of Sciences of the United States of America* 98(26): 15149-15154.

Koltai H & Weingarten-Baror C. (2008). "Specificity of DNA microarray hybridization: characterization, effectors and approaches for data correction." *Nucl. Acids Res.*;36 (7):2395-2405.

Epstein, J. R. & I. Biran, et al. (2002). "Fluorescence-based nucleic acid detection and microarrays." *Analytica Chimica Acta* 469(1): 3-36.

Li, Q., G. Luan, et al. (2002). "A new class of homogeneous nucleic acid probes based on specific displacement hybridization." *Nucl. Acids Res.* 30(2): e5.

DeRisi, J. *et al*. (1996). ''Use of a cDNA microarray to analyse gene expression patterns in human cancer." *Nat. Genet.* 14, 457−460.

Nicewarner-Pena, S.R. *et al*. (2001). "Submicrometer metallic barcodes." *Science* 294, 137−141.

Chan, W.C. *et al*. (2002). "Luminescent quantum dots for multiplexed biological detection and imaging." *Curr. Opin. Biotechnol.* 13, 40−46.

Dunbar, S. A. (2006). "Applications of Luminex® xMAP(TM) technology for rapid, high-throughput multiplexed nucleic acid detection." *Clinica Chimica Acta* 363(1-2): 71-82.

Liu, J. ; Lu, Y. *J.* (2005). " Stimuli-responsive disassembly of nanoparticle aggregates for light-up caloremetric sensing.'' *J. Am. Chem. Soc.* 127, 12677-12683

Porschke, D. & Eigen, M. (1971). "Co-operative nonenzymic base recognition. III. Kinetics of the helix-coil transition of the oligoribouridylic * oligoriboadenylic acid system and of oligoriboadenylic acid alone at acidic pH." *J. Mol. Biol*. 62, 361-381.

F. J. Isaacs et al. (2004). "Engineered riboregulators enable post-transcriptional control of gene expression." *Nat. Biotechnol*, 22, 841.

L. Qian & E. Winfree. (2009). "A simple DNA gate motif for synthesizing large-scale circuits." in DNA Computing, pp. 70–89

J.J. Li & W. Tan. (2002). "A single DNA molecular motor." *Nano Letters, 315-318*

C.K. Tison & V.T. Milam. (2007). “Reversing DNA-mediated adhesion at a fixed temperature.” *Langmuir,* 23 (19) 9728-9736

S.T. Parpart, C.K. Tison, V.T. Milam. (2010). “Effects of mismatches on DNA as an isothermal assembly and disassembly tool.” *Soft Matter*, 6 3832-3840